Mullins effect in a filled elastomer under uniaxial tension

A. Maiti,* W. Small, R. H. Gee, T. H. Weisgraber, S. C. Chinn, T. S. Wilson, and R. S. Maxwell
Lawrence Livermore National Laboratory, Livermore, California 94550, USA
(Received 3 October 2013; published 16 January 2014)

Modulus softening and permanent set in filled polymeric materials due to cyclic loading and unloading, commonly known as the Mullins effect, can have a significant impact on their use as support cushions. A quantitative analysis of such behavior is essential to ensure the effectiveness of such materials in long-term deployment. In this work we combine existing ideas of filler-induced modulus enhancement, strain amplification, and irreversible deformation within a simple non-Gaussian constitutive model to quantitatively interpret recent measurements on a relevant PDMS-based elastomeric cushion. We find that the experimental stress-strain data is consistent with the picture that during stretching (loading) two effects take place simultaneously: (1) the physical constraints (entanglements) initially present in the polymer network get disentangled, thus leading to a gradual decrease in the effective cross-link density, and (2) the effective filler volume fraction gradually decreases with increasing strain due to the irreversible pulling out of an initially occluded volume of the soft polymer domain.

DOI: 10.1103/PhysRevE.89.012602 PACS number(s): 61.41.+e, 61.80.−x, 62.20.−x, 76.60.−k

I. INTRODUCTION

Poly(dimethylsiloxane) (PDMS), with strong resistance to high temperature, radiation, and chemical attack, is the most widely used silicone elastomer in many applications ranging from artificial organs and biomedical devices to cushions, coatings, adhesives, interconnects, and seismic-isolation, thermal, and electrical barriers [1–11]. However, to ensure consistent performance under long-term deployment, one needs to carefully examine cumulative effects that might potentially alter its properties of interest. With our focus on the mechanical properties of PDMS-based cushion and support pads, we have previously examined the effect of radiation on the molecular weight distribution, cross-link density, elastic modulus, and permanent set in cross-linked PDMS elastomers of our interest [12,13]. We found that in all these experiments, the effect of radiation is strongly coupled with mechanical softening and permanent set effects due to repeated cycling of the rubber [14], a well-known effect commonly called the Mullins effect [15,16]. In applications where the amount of radiation exposure is small, it is important to develop a quantitative theory to understand and estimate the changes in elastic modulus and permanent set due to the Mullins effect.

The Mullins effect typically has the following characteristic signatures [15–17]: (1) significant softening results upon the first unloading cycle; (2) the amount of softening increases with increase in the maximum strain in the first cycle; (3) subsequent loading closely follows the first unloading curve and the unloading shows much less softening as long as the previous maximum strain is not exceeded; (4) if a subsequent loading exceeds the previous maximum, it acts as if to follow a continuation of the previous maximum loading curve; (5) there can be an induced anisotropy even in rubber that is isotropic in its virgin state; and (6) there is often a small but noticeable permanent set at the end of the first unloading curve. The permanent set typically increases upon unloading from an increased maximum strain, although in some cases it can recover after a long resting time [18]. Although the Mullins effect has been observed in both filled and unfilled rubber, it is particularly pronounced in systems with significant filler content, and although most studies have involved uniaxial tension, there have been a few studies under more general loading conditions [19,20].

Analysis by many groups over the past several decades has led to the suggestion of several different physical mechanisms behind the Mullins effect, including polymer-filler chain breakage [21–23], chain slippage [24,25], rupture of filler clusters [26], and chain disentanglement [27]. Although the detailed mechanism is not clear, and perhaps could even be dependent on the type of rubber, filler, strain rate, etc., many authors have taken the viewpoint that stiff filler particles lead to an enhanced elastic modulus through rubber-filler attachments that provide additional restrictions on the cross-linked rubber network—softening results from the breakdown, slippage, or loosening of some of these attachments, a phenomenon commonly referred to as *stress softening* [22–31]. Modeling such phenomenon has typically involved the representation of filled rubber with multiple networks, and strain-induced damage or alteration of one of the networks, while more detailed refinements, e.g., that involving the cluster topology of fillers, are progressively being introduced [32,33]. An alternative way to analyze Mullins effect has been to treat filled rubber as a system comprised of soft and hard domains [34–40] that evolve under stretch—softening is caused by the quasi-irreversible increase in the volume fraction of the soft domain. Models based on the second line of thought [41,42] postulate a localized nonaffine deformation of the molecular networks due to short chains reaching their limits of extensibility, and effective *strain amplification* [35–37] in the soft domain as compared to the actually applied strain because of almost zero strain in the hard domain.

The first viewpoint of describing Mullins effect typically necessitates complex materials-based models that continue to get refined in the current literature [32,33,43]. Such developments are important because they can quantitatively relate observed effects like strain-induced anisotropy, permanent set, and inelastic response to physical assumptions of network damage like chain sliding on and debonding from filler aggregates. On the other hand, the second viewpoint (i.e.,

*Corresponding author: amaiti@llnl.gov

strain amplification) is more phenomenological [41] and easier to implement numerically. However, there is some ambiguity in how strain should be amplified. For instance, Mullins and Tobin [34,35] suggested amplifying the uniaxial strain, Govindjee and Simo [28] suggested amplifying the total deformation gradient, while Boyce and co-workers [41,42] have suggested amplifying the first invariant of stretch I_1. One could also construct more realistic models that incorporate nonuniformity of strain enhancement, e.g., through the inclusion of microstrain gradient [44].

In this paper we analyze the observed Mullins softening in a filled PDMS rubber material of our interest using the concept of strain amplification in a way originally proposed by Mullins and Tobin [34,35]. Given the large amounts of stretch involved, we adopt a non-Gaussian stress function [45,46] and generalize it for the case of amplified strain. The layout of the paper is as follows: Sec. II contains a short discussion of the experimental measurements, Sec. III systematically develops the materials model, Sec. IV summarizes the main results, and we conclude with a brief summary in Sec. V.

II. MEASUREMENTS

The mechanical measurements reported here were performed on the commercial silicone elastomer TR-55 from Dow Corning, the same system on which previous studies of radiation aging had been carried out [12–14,47]. It essentially consists of silicone gum stock (primarily PDMS) filled with 30 wt % of fumed silica, which corresponds to a filler volume fraction of ∼16%. In our mechanical measurements, rectangular samples (∼3 mm wide by ∼1 mm thick) of TR-55 were stretched to a maximum engineering strain of $\varepsilon_{\max} \sim 2.15$ at a rate of 20 mm/min under ambient conditions. The initial grip separation was 20 mm. After 5 s at $\varepsilon_{\max}$ the external stretching force was removed and the samples relaxed to a state of equilibrium (i.e., zero stress). After 5 s in the zero stress condition, the samples were stretched again to the previously attained maximum stretch. The cycle was repeated four times. During the fifth loading cycle, the sample was stretched beyond the previous maximum stretch. Figure 1 plots

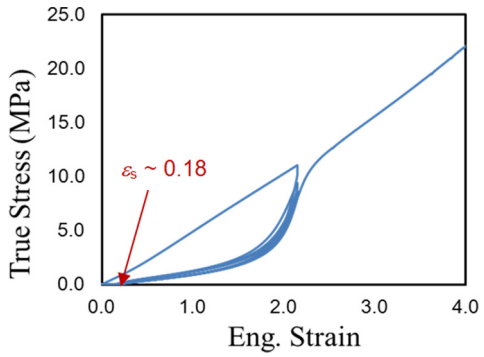

FIG. 1. (Color online) Stress-strain curve for a typical TR-55 sample that underwent five loading and four unloading cycles with the first four loading cycles limited to an engineering strain of 2.15 and the fifth loading cycle exceeding this strain. In addition to the typical Mullins softening, one observes a large permanent set with a recovered engineering strain $\varepsilon_s \sim 18\%$.

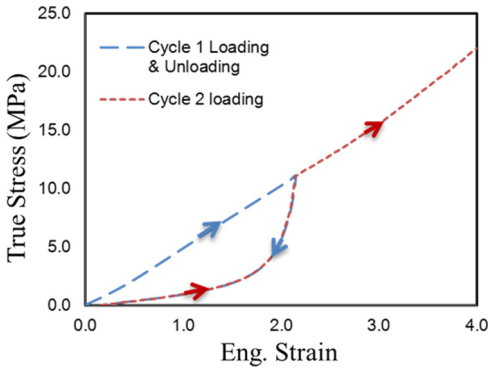

FIG. 2. (Color online) A simplified representation of Fig. 1 for modeling purpose.

the stress-strain response of a typical TR-55 sample. It exhibits many of the characteristic Mullins signatures mentioned in the Introduction. Two aspects that are most noteworthy are the significant softening and a large permanent set incurred upon the very first unloading, with a recovered engineering strain $\lambda_s - 1 \sim 18\%$ (where λ_s is the ratio of the length of the specimen with incurred permanent set to the original length). If such strain levels are not accounted for prior to the deployment of the elastomeric component in mechanical support devices, it can have undesired effects in the long-term performance.

III. MODELING

Given that the difference between the first unloading curve and subsequent loading and unloading curves are small until the previous maximum strain is exceeded, a common simplification is to ignore such difference, as illustrated in Fig. 2. Thus, a quantitative analysis of the Mullins effect becomes an exercise in describing the first loading and the first unloading curves for varying maximum strain levels. In order to develop an appropriate stress-strain relation, i.e., a materials model, we start from the simple neo-Hookean model [46] often employed in the description of the mechanical response of unfilled, cross-linked rubber. Under a uniaxial strain, the expression for stress in this model is given by

$$\sigma(\lambda) = G_0(\lambda^2 - 1/\lambda), \tag{1}$$

where σ is the true stress, λ is the stretch ratio (i.e., $\lambda = 1 + \varepsilon$, where ε is the engineering strain), and G_0 is the shear modulus. For an unfilled network system G_0 can be expressed as a function of the cross-link density, with some dependence on the network topology, junction coordination, etc. [48]. The above model is based on the assumption that the cross links behave essentially as Gaussian chains, which can be justified under not-too-large strains. Under large strains finite extensibility needs to be taken into account via non-Gaussian statistics, under which Eq. (1) gets modified to the Wang-Guth model [45,46]:

$$\sigma(\lambda) = \frac{1}{3}G_0\sqrt{N}\left\{\lambda L^{-1}(\lambda/\sqrt{N}) - \frac{1}{\sqrt{\lambda}}L^{-1}(1/\sqrt{\lambda N})\right\}, \tag{2}$$

where N is a parameter describing the finite chain length of the small-chain cross links (presumably related to polymer-filler

attachments), and L^{-1} is the inverse of the Langevin function given by $L(x) = \coth(x) - 1/x$. In the small strain limit, where $\lambda/\sqrt{N} \ll 1$ (assuming $N \gg 1$), the inverse Langevin function can be approximated as $L^{-1}(\lambda/\sqrt{N}) \approx 3\lambda/\sqrt{N}$, and Eq. (2) reduces to Eq. (1).

The Wang-Guth model, Eq. (2), is suitable for describing the mechanical response of networked, elastomeric systems without fillers. For filled systems, Mullins and later workers found it necessary to incorporate the notion of strain amplification. To represent strain amplification we follow the original work of Mullins and Tobin [34,35] and replace the stretch ratio λ in Eq. (2) by an amplified stretch ratio Λ given by

$$\Lambda = 1 + X(\lambda - 1), \tag{3}$$

where X is an amplification factor that depends on the *effective* volume fraction v_{eff} of the hard domain, i.e., fillers. A commonly used form for X as a function of v_{eff} is given by [42]

$$X = 1 + 3.5v_{\text{eff}} + bv_{\text{eff}}^2. \tag{4}$$

In Eq. (4) b is a parameter with a commonly used value of 18, which is obtained by comparing with the widely adopted filler-enhancement model due to Guth and Gold [49] that is applicable for well-dispersed nearly spherical filler particles with not-too-high volume fraction ($\approx$15% or below). In reality, even at this filler fraction silica or carbon-black filler particles can be nonuniformly distributed with significant clustering, which will necessitate modification of Eq. (4). However, for simplicity, we will continue to use Eq. (4) (with $b = 18$) and an assumption of spatially uniform strain amplification (i.e., no microstrain gradient [44]) with the implicit understanding that any correction due to these effects is absorbed within other factors, e.g., G_0 and v_{eff}.

Replacing the stretch ratio λ in Eq. (2) by Λ, and accounting for the fact that the elastic response comes only from the soft part of the material, we obtain the following materials model for filled rubber:

$$\sigma(\lambda) = \frac{1}{3}(1 - v_{\text{eff}})G_0\sqrt{N}\left\{\Lambda L^{-1}(\Lambda/\sqrt{N}) - \frac{1}{\sqrt{\Lambda}}L^{-1}(1/\sqrt{\Lambda N})\right\}. \tag{5}$$

Equation (5) can be used to describe the Mullins effect quantitatively by assuming that during the first loading curve the soft part of the matrix is being pulled out of the hard region thus progressively decreasing the relative volume fraction v_{eff} of the hard domain. The volume fraction of the soft part $(1 - v_{\text{eff}})$ should increase monotonically with an increase in the maximum strain level, and expected to reach a saturation value depending upon the relative amount of filler particles that was originally mixed into the rubber formulation.

Finally, to account for the observed permanent set (see Fig. 1) the formula for stretch ratio, Eq. (3), was modified as follows:

$$\Lambda = 1 + X\left(\frac{\lambda}{\lambda_s} - 1\right), \tag{6}$$

where λ_s is the recovered length, which in our model is assumed to increase linearly with λ during the first loading cycle until a maximum value of $\lambda_{s,\max}$ is reached at the maximum strain. During any subsequent unloading and reloading λ_s remains constant at this maximum value until the previously attained maximum strain is exceeded. The numerical value of $\lambda_{s,\max}$ is obtained from the experimental recovered length at the end of the first unloading curve. More specifically, λ_s is assumed to be of the form

$$\lambda_s = 1 + C(\lambda - 1) \tag{7}$$

or

$$\lambda_s = 1 + C(\lambda_{\max} - 1), \tag{7'}$$

where Eq. (7) applies during the first loading, or any subsequent loading beyond the previously attained maximum strain $\lambda_{\max}$, while Eq. (7') applies during unloading or subsequent loading at strain levels below $\lambda_{\max}$. The constant C is determined from the measurement of permanent set upon unloading from a moderate or large value of $\lambda_{\max}$, e.g., from Fig. 1, $\lambda_s = 1.18$ for $\lambda_{\max} = 3.15$, which yields $C \sim 0.084$ for our system. Equations (4)–(7) constitute the materials model employed in the simulations presented below.

IV. RESULTS

In order to compute the stress-strain behavior $\sigma(\lambda)$ using the model developed in the previous section, the parameters G_0, b, N, v_{eff}, and λ_s need to be determined. The motivation of this project was to obtain these parameters (some of which could vary with the applied strain ε if necessary) such that not only is the computed stress in quantitative agreement with that observed experimentally for TR-55 (Fig. 1), but also the parameters conform with previous knowledge about similar filled systems. For instance, given ~16% volume fraction of fillers in TR-55, the parameter b is expected to be ~18 [42,49], while the filler-enhancement factor at low stress should be roughly in the range 2–4 (Fig. 4, Ref. [41]). From the phantom network model G_0 can be assumed proportional to the cross-link density ($\nu_{x\,\text{link}}$) through the equation $G_0 = \nu_{x\,\text{link}}(1 - 2/f_c)k_BT$ [48], where f_c is the average network coordination, k_B is the Boltzmann constant, and T is the absolute temperature. However, there is always a degree of uncertainty as to the nature of the cross link, e.g., a chemical cross link vs a physical entanglement. Swelling experiments on unfilled systems of similar polymeric material indicate that the chemical cross-link density is much too small (by a factor of ~4–5) to account for the observed mechanical modulus at low strain. This leads us to believe that prior to being subjected to any strain, the polymer chains in the TR-55 material are strongly entangled, while upon swelling or mechanical stretching a significant fraction of these entanglements become disentangled, thus reducing the effective value of G_0.

Figure 3 (dashed-dotted curve) displays the results of our model calculation of true stress (σ) as compared to the experimental data from Fig. 1 (up to a maximum engineering strain of $\varepsilon = 2.15$). The various parameters, chosen within the constraints mentioned in the previous paragraph, were $b = 18$; $N = 30$; $\lambda_s = 1$ at $\varepsilon = 0$ increasing linearly to $\lambda_s = 1.18$ at the end of loading ($\varepsilon = 2.15$); G_0 starting from an original value of $G_{0,\text{orig}} = 0.35$ MPa at zero strain (point A: $\varepsilon = 0$) decreasing linearly to 25% of this initial value at the

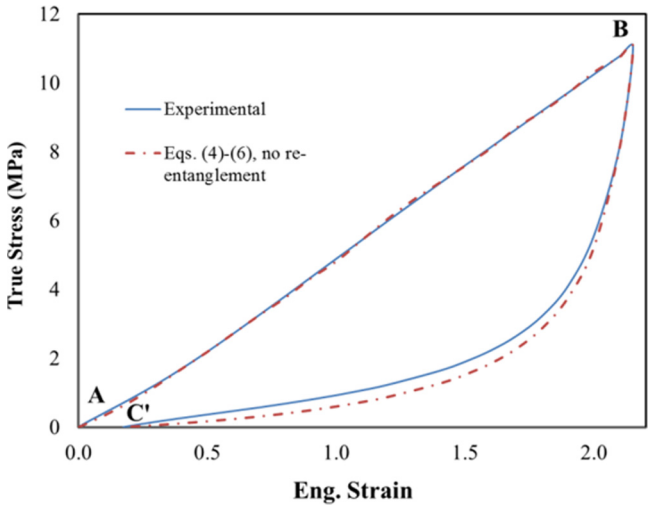

FIG. 3. (Color online) Stress-strain response in TR-55 during the first loading-unloading cycle (maximum engineering strain $\varepsilon_{max} = 2.15$): Experimental vs simulated results. The experimental results are from Fig. 1, while the simulated results are obtained using Eqs. (4)–(6) (see text) with no re-entanglements allowed during unloading (see Fig. 5). The simulated curve corresponds to fixed parameters $b = 18$, $N = 30$; on the loading curve G_0 decreases linearly from 0.35 MPa at point A to 0.09 MPa at point B and then assumed to remain constant during unloading (path BC′) and further loading until the previous maximum strain is exceeded.

end of loading (point B: $\varepsilon = 2.15$). The gradual decrease in G_0 during the loading corresponds to a fourfold decrease in the effective cross-link density due to detangling of physical entanglements, as discussed in the previous paragraph. The value of v_{eff}, the effective volume of the hard domain, was treated as an adjustable parameter so that the computed stress $\sigma(\lambda)$ follows the experimental loading curve.

Figure 4 displays the resulting behavior of v_{eff} as a function of strain. Although the actual volume fraction of the fillers is only ~16% in TR-55, v_{eff} starts out higher, around 42%. The

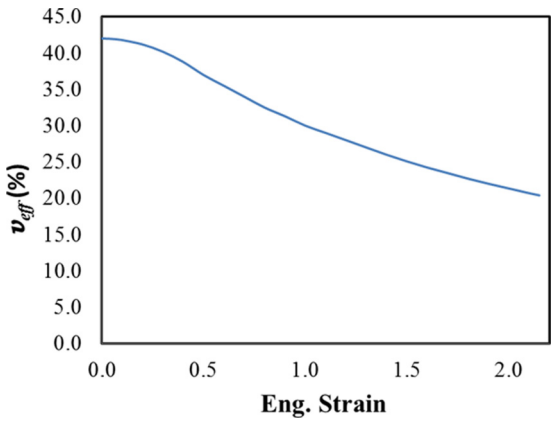

FIG. 4. (Color online) The *effective* volume of the hard domain v_{eff} as a function of strain during the first loading curve. During subsequent loading and unloading cycles v_{eff} in this model is assumed to remain at its lowest value (achieved during the previous maximum loading) until the previously attained maximum strain level is exceeded.

higher than actual value of v_{eff} in the beginning of loading can be interpreted as due to an occluded volume of the polymer that effectively behaves like part of the rigid domain [50]. With increasing strain, this occluded volume gets released, thus irreversibly increasing the fraction of the soft domain and correspondingly decreasing the volume fraction of the hard domain. At large strains, one expects the occluded volume to nearly go to zero, in which case v_{eff} should be around the volume fraction of the fillers originally included in the rubber formulation, consistent with the behavior we see in Fig. 4. Another point of consistency check for this model is to consider the filler-enhancement factor for the mechanical modulus at small strain. By comparing the small-strain limit of Eq. (1) [or (2)] with that of the strain-amplified materials model [Eq. (5)] one obtains the following formula for the enhancement factor (denoted by α):

$$\alpha = (1 - v_{\text{eff}})X = (1 - v_{\text{eff}})\left(1 + 3.5v_{\text{eff}} + bv_{\text{eff}}^2\right). \quad (8)$$

which, with the choice of $b = 18$, reduces to the well-known filler-enhancement factor of Guth and Gold [49]. Using the small-strain value $v_{\text{eff}} \sim 0.42$ (see Fig. 4), we obtain $\alpha \sim 3.3$, which is within the range expected from experimental values on a number of filled rubber systems (Fig. 4, Ref. [41]).

We note that in Fig. 3 the computed unloading curve consistently falls below the experimental unloading curve. The origin of this could be traced back to the assumption in our model that the initially occluded volume of the soft domain that gets pulled out and the physical entanglements that get detangled during the application of tensile strain are both irreversible, i.e., there is no recovery in either of these quantities during the unloading process. Allowing partial recovery in either or both of these quantities will result in a simulated stress that is much closer to the experimental value. Given that possible retraction of the occluded volume presumably occurs on a much longer time scale than the experimental times, we have considered below the case in which the soft network domain undergoes some physical entanglement during unloading. Figure 5 displays the behavior of the modulus G_0 (as a fraction of the starting value) during loading and unloading in situations both with and without re-entanglement. The case with re-entanglement leads to the computed stress-strain curve overlap with the experimental data, as shown in Fig. 6.

Finally, from the above model it is straightforward to simulate the stress-strain behavior for any loading-unloading cycle with a maximum strain level within the maximum in Fig. 3 (i.e., $\varepsilon_{max} \leq 2.15$). Figure 7 (top) displays the simulated results for four loading-unloading cycles with $\varepsilon_{max} = 0.5$, 1.0, 1.5, and 2.15, respectively. As alluded to in Fig. 2, in our model the unloading curve of the previous cycle coincides with the loading curve of the following cycle. This simulated result can be directly compared with experimentally measured stress-strain data [Fig. 7 (bottom)], where it was necessary to use a different sample (cut out of the same original TR-55 material) because the one used in Fig. 1 had been permanently altered.

V. SUMMARY

In this paper we have developed a phenomenological model that quantitatively reproduces the stress-strain behavior

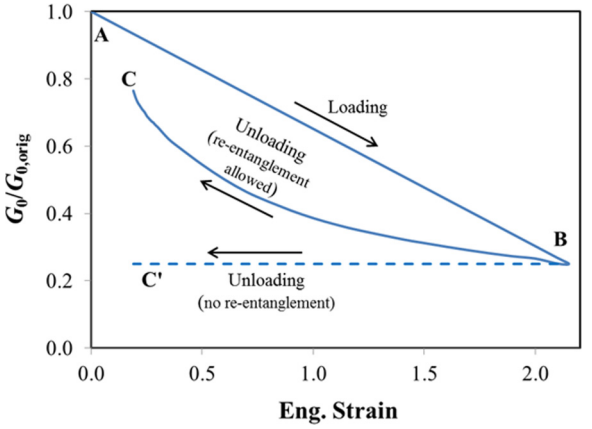

FIG. 5. (Color online) The behavior of modulus G_0 (which can be assumed proportional to the density of cross links in the soft domain, both physical and chemical) as a function of the applied strain during the first loading and unloading cycle. For unloading two different paths are shown: no re-entanglement allowed (dashed curve BC′) that leads to curve BC′ in Fig. 3; and re-entanglement allowed (solid curve BC) that leads to curve BC in Fig. 6. A large fraction of the physical entanglements lost during loading appear to get recovered by the end of unloading.

of a specific filled rubber system (TR-55). The model is based on using the Mullins-Tobin concept of amplified strain within the Wang-Guth stress function and is based on the following assumptions: (1) The permanent set (expressed as recovered length λ_s) increases linearly as a function of the maximum strain level reached up to that point; (2) modulus G_0, assumed proportional to an effective cross-link density decreases linearly as a function of the loading strain due to the detangling of physical entanglements, with partial recovery during unloading; and (3) the effective volume of the soft part $(1 - v_{\text{eff}})$ increases monotonically with the loading strain (due to the gradual pulling of the soft polymer domain out of an initially occluded phase) until a saturation value depending on the relative amount of filler is reached. The

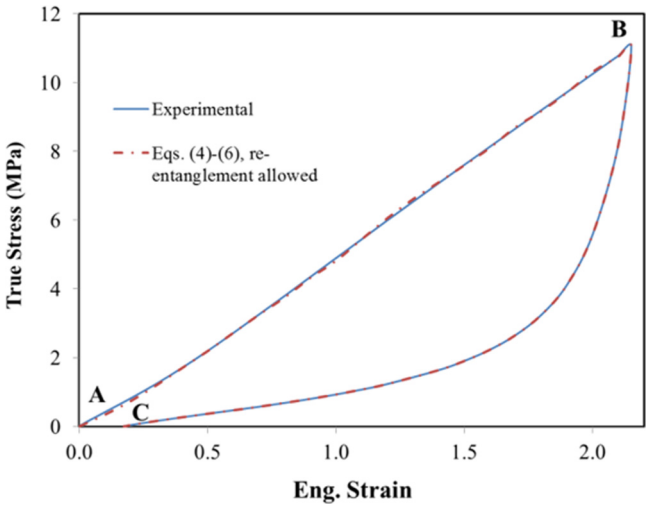

FIG. 6. (Color online) The same as Fig. 3 with re-entanglement upon unloading allowed (see path BC in Fig. 5).

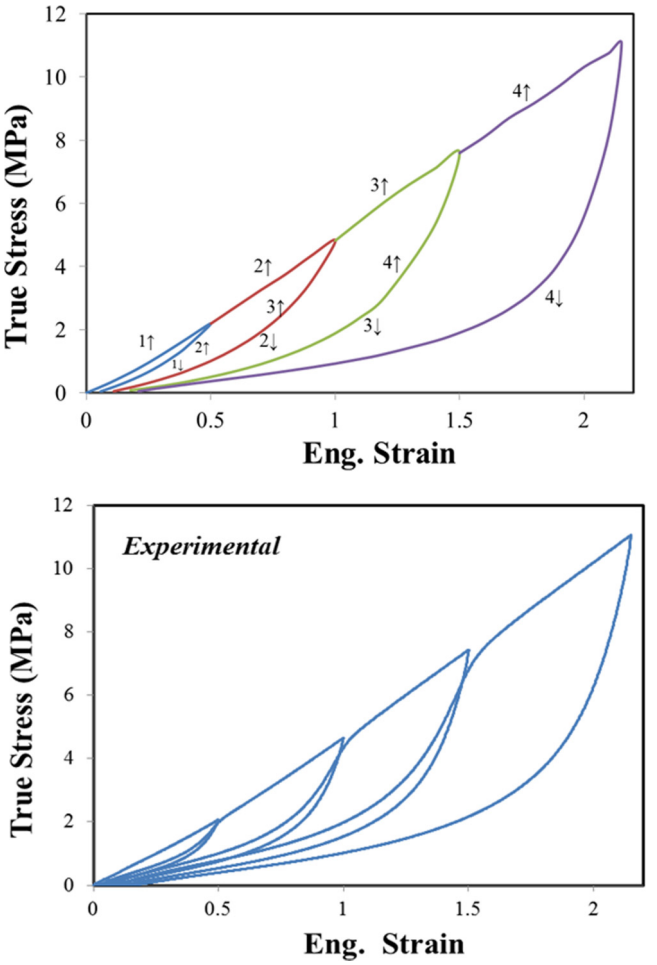

FIG. 7. (Color online) (Top) Simulated stress-strain response in TR-55 for different intermediate maximum strain levels: Cycle 1 ($\varepsilon_{\max} = 0.5$); cycle 2 ($\varepsilon_{\max} = 1.0$); cycle 3 ($\varepsilon_{\max} = 1.5$); and cycle 4 ($\varepsilon_{\max} = 2.15$). The loading (unloading) segments are indicated with up (down) arrows. The model parameters employed are the same as used to obtain the simulated results in Fig. 6. (Bottom) Corresponding experimental loading-unloading data through four cycles. A sample different from the one used in Fig. 1 (cut out of the same original TR-55 material) was employed in these measurements.

model yields a small-strain filler-enhancement factor of 3.3 for our system with 16 vol % filler, which is within the range of what has been reported in the literature for a number of different filled rubber systems at such filler content. However, the model developed here is for uniaxial strain only. It would be interesting to generalize it to other types of deformations, e.g., biaxial loading or shear, which would likely involve expressing amplification in terms of one or more invariants of strain [41].

ACKNOWLEDGMENT

This work was performed under the auspices of the US Department of Energy by Lawrence Livermore National Laboratory under Contract DE-AC52-07NA27344.

[1] J. E. Mark, B. Erman, and F. R. Eirich (eds.), *Science and Technology of Rubber* (Academic, New York, 2005).
[2] C. A. Harper (ed.), *Handbook of Plastics, Elastomers, & Composites* (McGraw-Hill, New York, 2002).
[3] A. Ciesielski, *An Introduction to Rubber Technology* (Rapra Technology, Shrewsbury, Shropshire, UK, 1999).
[4] M. J. Owen, *Siloxane Polymers*, 1st ed. (Prentice Hall, Englewood Cliffs, NJ, 1993).
[5] R. Morent *et al.*, J. Phys. D: Appl. Phys. **40**, 7392 (2007).
[6] L. H. U. Andersson and T. Hjertberg J. Appl. Polym. Sci. **88**, 2073 (2003).
[7] K. H. Wu, C. M. Chao, T. F. Yeh, and T. C. Chang, Surf. Coat. Technol. **201**, 5782 (2007).
[8] J. K. Pike, T. HoKenneth, and K. Wynne, Chem. Matter **8**, 856 (1996).
[9] F. Buyl, Int. J. Adhes. **21**, 411 (2001).
[10] Y. Ikada, Biomaterials **15**, 725 (1994).
[11] F. Abbasi, H. Mirzadeh, and A. Katbab, Polym. Int. **51**, 882 (2002).
[12] A. Maiti, T. Weisgraber, L. N. Dinh, R. H. Gee, T. Wilson, S. Chinn, and R. S. Maxwell, Phys. Rev. E **83**, 031802 (2011).
[13] L. Dinh, B. P. Mayer, A. Maiti, S. Chinn, and R. S. Maxwell, J. App. Phys. **109**, 094905 (2011).
[14] A. Maiti, T. H. Weisgraber, R. H. Gee, W. Small, C. T. Alviso, S. C. Chinn, and R. S. Maxwell, Phys Rev. E **83**, 062801 (2011).
[15] L. Mullins, Rubber Chem. Technol. **21**, 281 (1948).
[16] L. Mullins, Rubber Chem. Technol. **42**, 339 (1969).
[17] J. Diani, B. Fayolle, and P. Gilormini, Eur. Polym. J. **45**, 601 (2009).
[18] M. Itskov, E. Haberstroh, A. E. Ehret, and M. C. Voehringer, KGK–Kaut. Gummi. Kunst. **59**, 93 (2006).
[19] M. F. Beatty and S. Krishnaswamy, Z. Angew. Math. Phys. **51**, 984 (2000).
[20] Y. Merckel, M. Brieu, J. Diani, and J. Caillard, J. Mech. Phys. Solids **60**, 1257 (2012).
[21] A. F. Blanchard and D. Parkinson, Ind. Eng. Chem. **44**, 799 (1952).
[22] F. Bueche, J. Appl. Polym. Sci. **4**, 107 (1960).
[23] F. Bueche, J. Appl. Polym. Sci. **5**, 271 (1961).
[24] R. Houwink, Rubber Chem. Technol. **29**, 888 (1956).
[25] H. Killian, M. Strauss, and W. Hamm, Rubber Chem. Technol. **67**, 1 (1994).
[26] G. Kraus, C. W. Childers, and K. W. Rollman, J. Appl. Polym. Sci. **10**, 229 (1966).
[27] D. E. Hanson *et al.*, Polymer **46**, 10989 (2005).
[28] S. Govindjee and J. C. Simo, J. Mech. Phys. Solids **39**, 87 (1991).
[29] G. Marckmann, E. Verron, L. Gornet, G. Chagnon, P. Charrier, and P. Fort, J. Mech. Phys. Solids **50**, 2011 (2002).
[30] G. Chagnon, E. Verron, G. Marckmann, and L. Gornet, Int. J. Solids Struct. **43**, 6817 (2006).
[31] R. W. Ogden and D. G. Roxburgh, Proc. R. Soc. London Ser. A **455**, 2861 (1999).
[32] R. Dargazany and M. Itskov, Int. J. Solids Struct. **46**, 2967 (2009).
[33] R. Dargazany and M. Itskov, Phys. Rev. E **88**, 012602 (2013).
[34] L. Mullins and N. R. Tobin, Rubber. Chem. Tech. **30**, 555 (1957).
[35] L. Mullins and N. R. Tobin, J. Appl. Polym. Sci. **9**, 2993 (1965).
[36] J. A. C. Harwood, L. Mullins, and A. R. Payne, J. Appl. Polym. Sci. **9**, 3011 (1965).
[37] J. A. C. Harwood and A. R. Payne, J. Appl. Polym. Sci. **10**, 315 (1966).
[38] M. A. Johnson and M. F. Beatty, Continuum Mech. Thermodyn. **5**, 301 (1993).
[39] R. Bonart, J. Macromol. Sci. B **2**, 115 (1968).
[40] M. Lee and M. Williams, J. Polym. Sci. Polym. Phys. Ed. **23**, 2243 (1985).
[41] J. S. Bergstrom and M. C. Boyce, Rubber. Chem. Technol. **72**, 633 (1999).
[42] H. J. Qi and M. C. Boyce, J. Mech. Phys. Solids **52**, 2187 (2004).
[43] X. Zhao, J. Mech. Phys. Solids **60**, 319 (2012).
[44] S. Tang, M. S. Greene, and W. K. Liu, J. Mech. Phys. Solids **60**, 199 (2012).
[45] M. C. Wang and E. Guth, J. Chem. Phys. **20**, 1144 (1952).
[46] L. R. G. Treloar, *The Physics of Rubber Elasticity* (Clarendon, Oxford, UK, 1975).
[47] R. S. Maxwell *et al.*, Polym. Degrad. Stability **94**, 456 (2009).
[48] R. H. Boyd and P. J. Phillips, *The Science of Polymer Molecules* (Cambridge University Press, Cambridge, UK, 1993).
[49] E. Guth and O. Gold, Phys. Rev. **53**, 322 (1938).
[50] A. I. Medalia and G. Kraus, *Science and Technology of Rubber*, edited by J. E. Mark, B. Erman, and F. R. Eirich (Academic, New York, 1994).